Self-organization in systems of self-propelled particles

Herbert Levine and Wouter-Jan Rappel
Department of Physics, University of California, San Diego, La Jolla, California 92093-0319

Inon Cohen
School of Physics and Astronomy, Raymond & Beverly Sackler Faculty of Exact Sciences, Tel-Aviv University, Tel-Aviv 69978, Israel
(Received 14 June 2000; published 18 December 2000)

We investigate a discrete model consisting of self-propelled particles that obey simple interaction rules. We show that this model can self-organize and exhibit coherent localized solutions in one- and in two-dimensions. In one-dimension, the self-organized solution is a localized flock of finite extent in which the density abruptly drops to zero at the edges. In two-dimensions, we focus on the vortex solution in which the particles rotate around a common center and show that this solution can be obtained from random initial conditions, even in the absence of a confining boundary. Furthermore, we develop a continuum version of our discrete model and demonstrate that the agreement between the discrete and the continuum model is excellent.

DOI: 10.1103/PhysRevE.63.017101 PACS number(s): 05.65.+b, 05.40.Fb, 05.60.Cd

Self-organization and pattern formation in systems of self-propelled entities are ubiquitous in nature. Examples can be found in a variety of fields and include animal aggregation [1], traffic patterns, [2] and cell migration [3]. Recently, the problem of flocking, in which a large number of moving particles (e.g., fish or birds) remain coherent over long times and distances, has attracted considerable attention [4]. A simulation of a simple numerical model by Vicsek *et al.* [5] in which each particle has a constant identical speed and a direction of motion that is determined by the average direction of its neighbors, revealed that an ordered phase exists, even in the presence of noise and disorder. A subsequent analysis of a continuum model by Toner and Tu [6] investigated this ordered phase further and derived conditions for its stability.

These models have in common that the flocks have infinite extent and, in simulations, fill the entire computational box. In reality, however, flocks have a finite size, with its density dropping sharply at the edge of the flock [7]. In this Brief Report we present a discrete model consisting of self-propelled interacting particles that obey simple rules. We show that self-organization in our model leads to coherent *localized* states in one dimension (1D) and in two dimensions (2D) that are stable in the presence of noise and disorder. Furthermore, we present a continuum version of our discrete model which is obtained by coarse-grain averaging the discrete equations. The continuum flock solutions in 1D agree very well with the discrete solutions and are characterized by having a finite extent with densities that drop off sharply at the edges. In 2D, we focus on a vortex state in which the particles are rotating around a common center and show that the discrete model and the continuum model agree well.

Our discrete particle model consists of N particles with mass m_i, position $\vec{x}_i$ and velocity $\vec{v}_i$. Each particle experiences a self-propelling force $\vec{f}_i$ with fixed magnitude α. To prevent the particles from reaching large speeds, a friction force with coefficient β is introduced. In addition, each particle is subject to an attractive force which is characterized by an interaction range l_a. This force is responsible for the aggregation of the particles. To prevent a collapse of the aggregate, a shorter-range repulsive force is introduced with interaction range l_r. Thus, the governing equations for each particle is

$$m_i \partial_t \vec{v}_i = \alpha \hat{f}_i - \beta \vec{v}_i - \vec{\nabla} U, \tag{1}$$

$$\partial_t \vec{x}_i = \vec{v}_i . \tag{2}$$

We have checked that our qualitative results are independent of the explicit form of the interaction potential and we have chosen here an exponentially decaying interaction:

$$U = \sum_{j \neq i} C_a \exp(-|\vec{x}_i - \vec{x}_j|/l_a) - \sum_{j \neq i} C_r \exp(-|\vec{x}_i - \vec{x}_j|/l_r), \tag{3}$$

where C_a, C_r determine the strength of the attractive and repulsive force, respectively. The direction of the self-propelling force can be chosen along the instantaneous velocity vector or, similar to the numerical model of Ref. [5], can be determined by aligning it with the average velocity direction of the neighboring particles:

$$\hat{f}_i = \hat{v}_i \quad \text{without averaging,} \tag{4}$$

$$\hat{f}_i = \sum_{j \neq i} \hat{v}_j \exp(-|\vec{x}_i - \vec{x}_j|/l_c) \quad \text{with averaging,} \tag{5}$$

where l_c is a correlation length.

Let us now present our simulation results of the discrete model. The model was integrated by solving Eqs. (1) and (2) using a simple Euler integration routine with timestep $\Delta t = 0.2$. The simplest coherent *localized* solution in our model is a 1D flock in which all particles move with constant velocity $v = \alpha/\beta$. An example of this solution is presented in Fig. 1 where we have plotted, as solid circles, the density defined as $\rho_i = 2/(x(i+1) - x(i-1))$ as a function of the position of the particle. The density can be seen to drop

 ©2000 The American Physical Society

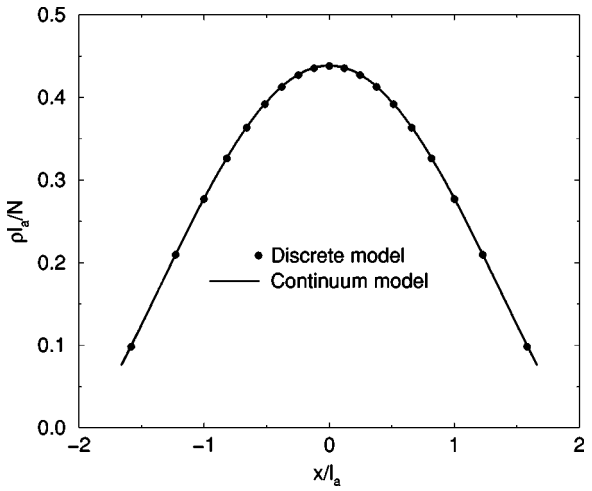

FIG. 1. A coherent moving flock in the one-dimensional version of the model with parameters (all with arbitrary units) $m=1$, $\alpha=0.5$, $\beta=1$, $C_a=0.45$, $l_a=60$, $C_r=2$, and $l_r=20$. The solid circles correspond to the solution of the discrete model for $N=200$ and every 10th particle displayed. The solid line shows the solution of the continuum model.

abruptly to zero at the edge of the flock. We have checked that this solution is stable in the presence of moderate amounts of noise [added to Eq. (2)] and of disorder in the parameters.

Further simulations revealed that increasing the number of particles does not change the shape of the density function and that the total size of the flock reaches a constant value. This is illustrated in Fig. 2 where the dashed line represents the size of the flock as a function of the number of particles. This obviously unrealistic behavior of the model is due to the soft-core repulsive force which allows the particles to be very close. Our model can easily be extended to incorporate

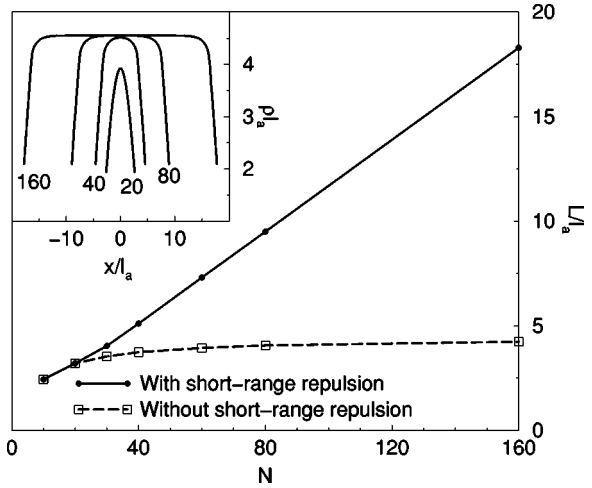

FIG. 2. The size L of a flock as a function of N with (solid line) and without (dashed line) an additional short-range hard-core potential. The inset shows the density of flocks in the presence of the short-range hard-core potential for different N. Parameter values: $m=1$, $\alpha=0.5$, $\beta=1$, $C_a=0.6$, $l_a=40$, $C_r=2$, $l_r=20$, $C_{hc}=1$, and $l_{hc}=10$.

hard-core repulsive forces. In fact, a flock with a size that scales approximately linearly with the total number of particles can be obtained by introducing a hard-core repulsive force in Eq. (1) [8]. The specific form of the hard-core potential is not important and we have chosen

$$U_{hc}=\sum_{j\neq i} C_{hc}(|x_i-x_j|-l_{hc})^5, \quad |x_i-x_j|\leqslant l_{hc},$$
$$U_{hc}=0, \quad |x_i-x_j|>l_{hc}. \tag{6}$$

In Fig. 2 we show, as a solid line, the size of the flock in the presence of this additional repulsive force as a function of N while in the inset we show the corresponding density of the flock for different N. Naturally, the force has only an effect when the interparticle separations are smaller than l_{hc}. Hence, for small N the flock solution is unaffected by the additional force. As N is increased and the interparticle spacing becomes smaller than l_{hc}, the particles in the center of the flock are pushed apart. For large N, the flock reaches a constant density in its center and its size scales linearly with N.

Let us now turn to 2D where we have obtained several flocking states. One, not shown here, is the equivalent of our 1D flock: all particles are moving in the same direction with $|\vec{v}_i|=\alpha/\beta$. The particles arrange themselves on a disk and this aggregate is stable under small amounts of noise and disorder. The solution which we will focus on here consists of a vortex state where the particles rotate around a common center and which is common in fish schools [9], bacterial colonies [10], and amoeba aggregates [11]. This solution has been observed previously in models of self-propelling particles but only in the presence of a confining boundary [12,13] or when a rotational chemotaxis term is invoked [10].

In our model, the vortex solution can be obtained from a wide variety of initial conditions including one in which all particles are randomly placed on a disk with speed α/β and random initial velocities. A typical evolution of the particles starting from this initial condition is shown in Fig. 3. This figure was obtained in the absence of the velocity averaging term and illustrates that in this case some particles move clockwise while the others rotate counter clockwise. When the velocity averaging term is included the final vortex state consists of all particles turning the same way. An example of this case is shown in the inset of Fig. 4. In both cases, the speed of each particle was found to be sharply peaked around $|\vec{v}|=\alpha/\beta$.

The average size of the vortex remains constant in time as shown in Fig. 4 where we have plotted the average density (obtained by averaging over 10^6 iterations) of the vortex structure. Figure 4 displays several remarkable features. First, there is a well-defined core which remains void even for extended simulation runs. Using different parameter values however, one can also produce a vortex without a core. Second, as in the one-dimensional flock, the density does not decay smoothly to zero at the edges. Instead, it increases at both the inner and outer edge of the aggregate and then drops

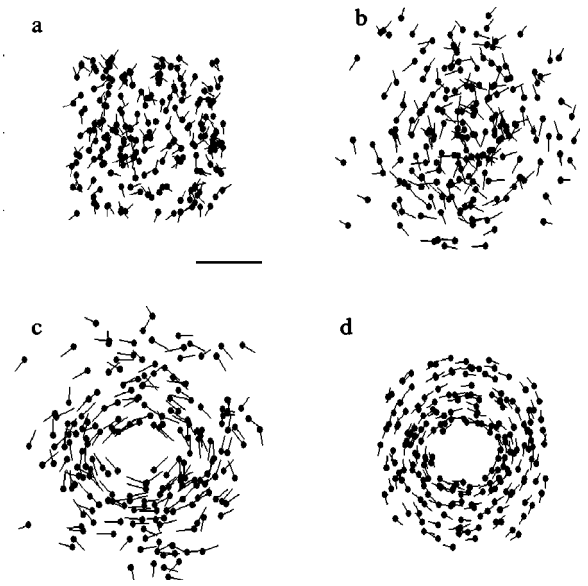

FIG. 3. Snapshots of $N=200$ particles for the parameter values $\alpha=10$, $\beta=1$, $l_c=0$, $C_a=0.4$, $l_a=40$, $C_r=1$, and $l_r=20$. As initial condition, the particles are placed at random on a disk with velocities that are constant in magnitude (α/β) but random in direction (a). After an initial transient [(b) 20 iterations and (c) 50 iterations], a stable rotating vortex state is formed [(d) 300 iterations]. The bar indicates the attraction length l_a. The position of each particle is denoted by a solid circle and the velocity as a line starting at the particle and pointing in the direction of the velocity.

abruptly. Qualitatively similar vortex solutions were found when an additional hard-core repulsion like the one discussed above is added.

As in the case of traffic models [14], it is useful to develop a continuum version of our model. To this end, we simply coarse-grain average the equations which results in,

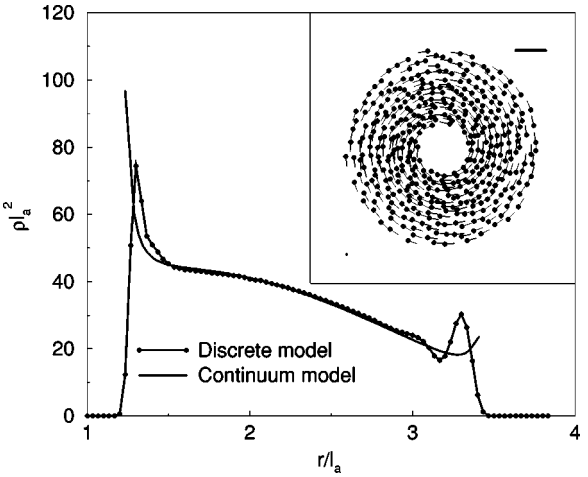

FIG. 4. Average density of a rotating vortex state in the discrete model (solid symbols) and the continuum model for the parameter values $N=400$, $m=1$, $\alpha=10$, $\beta=1$, $l_c=0$, $C_a=0.5$, $l_a=30$, $C_r=1$, and $l_r=20$. The inset shows a snapshot of the discrete model simulation with the bar corresponding to l_a. As initial condition we used a vortex obtained with $l_c=4$ which ensured that the angular velocity of all particles has the same sign.

after dividing by a common factor of ρ,

$$\partial_t \vec{v} + (\vec{v}\cdot\vec{\nabla})\vec{v} = \alpha\hat{f} - \beta\vec{v} + \vec{G} \tag{7}$$

together with the conservation equation for the density ρ

$$\partial_t \rho + \vec{\nabla}\cdot(\vec{v}\rho) = 0.$$

The interaction force is given by

$$\vec{G}(\vec{x}) = \int \rho(\vec{x}')\vec{\nabla} U(\vec{x},\vec{x}')d\vec{x}' \tag{8}$$

and the self-propulsive force direction is given by either

$$\hat{f}(\vec{x}) = \int \rho(\vec{x}')\hat{v}(\vec{x}')\exp(-|\vec{x}-\vec{x}'|/l_d)d\vec{x}' \tag{9}$$

in the velocity averaging case or simply by $\hat{f}=\vec{v}/|\vec{v}|$ otherwise.

A comparison between the discrete model and the continuum model can be carried out for the solutions presented here. For a 1D flock, we have simply $\hat{f}_i=1$, and the solution in the continuum model is given by $G=0$ or

$$\int \rho(x')U(x,x')dx' = D, \tag{10}$$

where D is a constant determining the total number of particles. Since the sought after solution has a finite extent with a discontinuity at the edge where the density drops to zero we discretize the integral using M points and discretization step Δx. The last point corresponds to the edge of the flock. The resulting linear set of M equations for ρ is easily solved using standard linear algebra packages, and Δx was varied until the slope at the center of the flock vanished. The result, with D chosen such that $\int \rho(x)dx = N$, is shown in Fig. 1 as a solid line. The density profile in the continuum model is discontinuous at the edge and agrees well with the profile obtained in the discrete model. Note that since the equations are linear in ρ it is not surprising to find that the density profile of the discrete model did not change as the number of particles is increased. Clearly, the simple coarse-grained averaging procedure is not adequate for the hard-core potential case, where higher order terms in the density are important.

The continuum model can also be used to find the vortex solution. To this end, we use the fact that all particles undergo approximately a circular motion with constant speed (α/β). Thus, a continuum vortex solution can be found by requiring that the force $\vec{G}$ is centripetal:

$$\int_0^{2\pi} d\phi \int_0^{\infty} dr'\, \rho(r')U(r,r',\phi) = D - (\alpha/\beta)^2 \ln(r). \tag{11}$$

After performing the integration over ϕ, the remaining integral was discretized as in the 1D case. The resulting matrix was solved for $\rho(r)$ and used in a Newton solver that searched for the size of the hole and the overall size of the vortex (i.e., discretization Δx) with a condition for smoothness of the solution at both discontinuous edges. This condi-

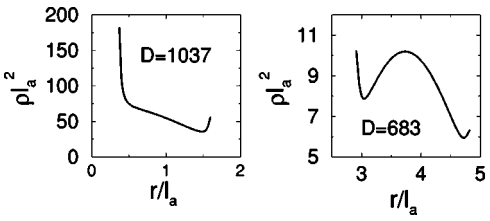

FIG. 5. Two different solutions of the continuum model for the parameters $\alpha/\beta=10, C_a=0.7, l_a=40, C_r=2, l_r=20$, and $N=200$.

tion simply consisted of requiring that the first and last point can be obtained by linear interpolation from its two neighboring points. We have checked that the solutions we obtained are converged by increasing the number of discretization points from 80 to 1480. In Fig. 4 we compare the discrete solution to the one obtained by Eq. (11) where the integration constant D was varied until $\int \rho(\vec{x})d\vec{x}=N$. Again, the continuum profile is discontinuous at the edges and the agreement between the continuum profile and the discrete profile is very good.

The continuum equation can be used to explore the (large) parameter space more efficiently. An example of such an exploration is shown in Fig. 5 where we plot two different solutions found by our Newton solver for the same model parameters and total number of particles ($N=200$) but with different integration constant D. Preliminary simulations of the discrete model show that the solution with the larger core is unstable and a formal stability analysis of the continuum solution will be carried out in the future.

In this Brief Report we have presented a model for localized aggregates and flocks. Our model contains very simple rules and can be straightforwardly extended to incorporate additional and different types of interactions. For example, the forces that maintain bacterial aggregates are believed to be short-range adhesion forces together with a short-range hard-core repulsion. The investigation of these types of interactions will be the subject of future work. Finally, it would be interesting to compare our results to animal flocks. Unfortunately, such a comparison is currently not possible since not enough quantitative data is available.

We acknowledge useful conversations with E. Ben-Jacob and W.F. Loomis. The work of H.L. and W.J.R. was supported in part by NSF Grant No. DBI-95-12809. I.C. acknowledges support from The Colton Scholarships and a Israeli–US Binational Science Foundation BSF grant.

[1] *Animal Groups in Three Dimensions*, edited by J. K. Parrish and W. Hamner (Cambridge University Press, Cambridge, 1997).

[2] I. Prigogine and R. Herman, *Kinetic Theory of Vehicular Traffic* (American Elsevier, New York, 1971).

[3] E. Ben-Jacob, I. Cohen, and H. Levine, Adv. Phys. (in press).

[4] N. Shimoyama *et al.*, Phys. Rev. Lett. **76**, 3870 (1996); A.S. Mikhailov and D.H. Zanette, Phys. Rev. E **60**, 4571 (1999); A. Czirok, A.-L. Barabasi, and T. Vicsek, Phys. Rev. Lett. **82**, 202 (1999); O.J. O'Loan and M.R. Evans, J. Phys. A **32**, L99 (1999).

[5] T. Vicsek *et al.*, Phys. Rev. Lett. **75**, 1226 (1995).

[6] J. Toner and Y. Tu, Phys. Rev. Lett. **75**, 4326 (1995); J. Toner and Y. Tu, Phys. Rev. E **58**, 4828 (1997).

[7] A. Mogilner and L. Edelstein-Keshet, J. Math. Biol. **38**, 534 (1999).

[8] It is of course also possible to eliminate the soft-core repulsive potential altogether. The soft-core repulsive potential is introduced here to facilitate a simple derivation of a continuum model.

[9] J.K. Parrish and L. Edelstein-Keshet, Science **284**, 99 (1999).

[10] E. Ben-Jacob, I. Cohen, A. Czirk, T. Vicsek, and D.L. Gutnick Physica A **238**, 181 (1997).

[11] W.-J. Rappel, A. Nicol, A. Sarkissian, H. Levine, and W.F. Loomis, Phys. Rev. Lett. **83**, 1247 (1999); A. Nicol, W.-J. Rappel, H. Levine, and W.F. Loomis, J. Cell. Sci. **112**, 3923 (1999).

[12] Y.L. Duparcmeur, H. Hermann, and J.P. Troadec, J. Phys. I **9**, 1119 (1995).

[13] J. Hemmingsson, J. Phys. A **28**, 4245 (1995).

[14] D. Helbing, Phys. Rev. E **53**, 2366 (1996).